

2012

## A simple route to carbon micro- and nanorod hybrid structures by physical vapour deposition

Jin Chu

*University of Puerto Rico*

Xiaoyan Peng

*University of Puerto Rico*

Ali Aldalbahi

*University of Wollongong, akma365@uowmail.edu.au*

Marc in het Panhuis

*University of Wollongong, panhuis@uow.edu.au*

Rafael Velazquez

*University of Puerto Rico*

*See next page for additional authors*

Follow this and additional works at: <https://ro.uow.edu.au/scipapers>



Part of the [Life Sciences Commons](#), [Physical Sciences and Mathematics Commons](#), and the [Social and Behavioral Sciences Commons](#)

---

### Recommended Citation

Chu, Jin; Peng, Xiaoyan; Aldalbahi, Ali; in het Panhuis, Marc; Velazquez, Rafael; and Feng, Peter X.: A simple route to carbon micro- and nanorod hybrid structures by physical vapour deposition 2012, 395102. <https://ro.uow.edu.au/scipapers/4543>

---

# A simple route to carbon micro- and nanorod hybrid structures by physical vapour deposition

## Abstract

Tilted well-aligned carbon micro- and nano-hybrid rods were synthesized on Si at different substrate temperatures and incident angles of carbon source beam using the hot filament physical vapour deposition technique. The morphologic surfaces, chemical compositions and bond structures of the oblique carbon rod-like structures were investigated by scanning electron microscopy, field emission scanning electron microscopy, transmission electron diffraction and Raman scattering spectroscopy. The field emission behaviour of the fabricated samples was also measured.

## Keywords

hybrid, structures, physical, simple, route, deposition, carbon, vapour, micro, nanorod

## Disciplines

Life Sciences | Physical Sciences and Mathematics | Social and Behavioral Sciences

## Publication Details

Chu, J., Peng, X., Aldalbahi, A., in het Panhuis, M., Velazquez, R. & Feng, P. X. (2012). A simple route to carbon micro- and nanorod hybrid structures by physical vapour deposition. *Journal of Physics D: Applied Physics*, 45 (39), 395102.

## Authors

Jin Chu, Xiaoyan Peng, Ali Aldalbahi, Marc in het Panhuis, Rafael Velazquez, and Peter X. Feng

# A Simple Route to Carbon Micro- and Nanorods Hybrid Structure by Physical Vapor Deposition

Jin Chu<sup>1</sup>, Xiaoyan Peng<sup>1</sup>, Ali Aldalbahi<sup>2</sup>, Marc in het Panhuis<sup>2</sup>, Peter.X.Feng<sup>1\*</sup>

*1 Institute of Functional Nanomaterials and Department of Physics, University of Puerto Rico, San Juan, Puerto Rico 00936, USA.*

*2 Soft Materials Group, School of Chemistry, and ARC Centre of Excellence for Electromaterials Science, University of Wollongong, Wollongong, NSW 2522, Australia.*

\*Corresponding author: Peter. X. Feng < p.feng@ upr.edu >

## Abstract:

Tilted well-aligned carbon micro- and nano- hybrid rods were synthesized on Si under different substrate temperatures and carbon source incident angles by using hot filament physical vapor deposition technique. The morphologic surfaces, chemical compositions and bond structures of the oblique carbon rod-like structures were investigated by scanning electron microscopy, field emission scanning electron microscopy, transmission electron diffraction and Raman scattering spectroscopy. The field emission behaviors of the fabricated samples were also measured.

**Keywords:** Carbon, Tilted rod-like structure, Physical vapor deposition, Field emission.

## 1. Introduction

One-dimensional carbon nanostructures (such as nanocones, nanotubes, nanoprisms and nanorods) have been widely studied as the next-generation cold cathodes candidates in field emission (FE) displays due to their unique electrical, chemical and mechanical properties [1–5]. The advantages of one-dimensional nanomaterials are their nanometer scale and high aspect ratio, so that they can be used as suitable field emitter or display device unit [6]. Carbon materials with high surface area have also been studied for hydrogen storage [7, 8]. A large number of carbon nanostructures have been obtained based on various techniques, including catalyst assisted solid-state growth process [9], reactive plasma beam sputtering [10], pulsed laser deposition (PLD) techniques [11,12], electron beam induced deposition [6, 13], chemical vapor deposition [14, 15], catalytic copyrolysis process [16] and benzene-thermal-reduction-catalysis route [17], etc..

Recently, one-dimensional tilted nanorods are attracting noticeable research interest due to their inherent anisotropic nature with the tilted geometry. Ye et al prepared tilted Si nanorod arrays using a two-phase substrate rotation method with the oblique angle deposition technique, which could produce nanorods with a controllable tilt angle [18]. We have synthesized one-dimensional carbon tilted nanorods by using the catalyst assisted oblique angle PLD technique [19]. However, these

---

\* Corresponding author. Tel.: +17877640000ext.2719; fax: +17877644063.  
E-mail address: p.feng@upr.edu (Peter. X. Feng).

methods are limited by the complicated fabrication process. So far, there is little information available for the synthesis of one dimensional tilted carbon microrods and nanorods.

In this work, we address a simple approach for synthesizing well aligned one-dimensional micro- and nanorods hybrid carbon structure by hot filament physical vapor deposition (HFCVD) technique. The growth process we describe here has two remarkable features: firstly, this method can produce uniformly tilted carbon micro- and nanorods with a controllable tilt angle; secondly, the experimental setup is simple and cost effective which satisfies the requirements of commercial applications.

## 2. Experimental setup

One-dimensional slanted carbon micro- and nanorods were synthesized on Si substrates using a simple HFCVD technique under different temperatures and incident angles. The easily-get graphite stick (0.7mm diameter, 15mm length) was used as a precursor to provide carbon source and filament, to replace the tungsten filament in our HFCVD system described elsewhere in our previous publications [20-22]. No catalyst or other carbon-containing compound precursor was used. Prior to the experiments, the substrates were ultrasonically washed in the methanol solution for 5mins, and dried with nitrogen. After placing the substrate, the chamber was pumped down to  $2.67 \times 10^{-3}$  Pa, then fed with Ar gas to ambient pressure and then pumped down to  $2.67 \times 10^{-3}$  Pa. Repeated this process 3 times to keep oxygen out and obtain a good vacuum. A dc power supply HY3020E with an electric current of 18A was used to heat the filament to a temperature of up to 2000°C to promote gas phase activation. The substrates were placed on a holder under the hot filament. No extra heater was used to heat the substrate holder. The temperature of the substrate was controlled by simply changing the distance between the substrate and the hot filament. The position of substrate on the holder can be changed to get different incident angle. The deposition duration was 30mins for all the samples.

The morphologic surface, chemical composition and bond structure of obtained samples were investigated by scanning electron microscopy (SEM) at 20KV, field emission scanning electron microscopy (FESEM) at 15KV, transmission electron diffraction (TED) at 15KV, and Raman scattering spectroscopy, respectively.

The FE measurements were carried out in a vacuum chamber at a pressure of  $\sim 4.0 \times 10^{-5}$  Pa at room temperature. A molybdenum rod of 3mm diameter (area:  $0.071 \text{ cm}^2$ ) serves as the anode. The macroscopic surface electric field ( $E_s$ ) on the sample (i.e. cathode) is estimated by  $E_s = V/d_{CA}$ , where  $V$  is the voltage applied to the anode and  $d_{CA}$  ( $100 \pm 2 \mu\text{m}$ ) is the distance between the anode and the cathode. The current was detected using a KEITHLEY 6517A electrometer. The power supply was a Stanford Research Systems PS350. A detailed description of the FE measurement techniques can be found in our previous papers [20, 23]

## 3. Results and discussions

Fig. 1 shows typical SEM images of the synthesized carbon samples (*a*, *b*, *c*) on Si substrates at temperature of (a) 800, (b) 900, (c) 1000°C, respectively. The insets are the cross section measured by JEOL JSM-7500F FESEM. The thickness of the samples is about 13.0 $\mu\text{m}$ , 19.2 $\mu\text{m}$ , 25.3 $\mu\text{m}$ , respectively. Different sized tail-like microrods were observed for the samples under different substrate temperatures (depend on distances), but otherwise identical growth conditions. At 800 °C,

the oblique rods with the angle of  $\sim 58^\circ$  to the normal of the substrate have a length of  $22.0\text{-}24.5\mu\text{m}$  and diameter  $0.6\text{-}0.7\mu\text{m}$  for their beginning part, and gradually increasing to  $1.0\text{-}1.5\mu\text{m}$  for the end part, which consist of several plume-like structures. Raising substrate temperature to  $900$  and  $1000^\circ\text{C}$ , similar structures but with larger size were obtained. The rod length was  $34.0\text{-}36.5\mu\text{m}$  and  $44.0\text{-}47.0\mu\text{m}$ , the beginning part diameter was  $0.65\text{-}0.75\mu\text{m}$  and  $0.7\text{-}1.0\mu\text{m}$ , then the diameter gradually increased to  $2.0\text{-}3.5\mu\text{m}$  and  $3.0\text{-}4.5\mu\text{m}$ , respectively.

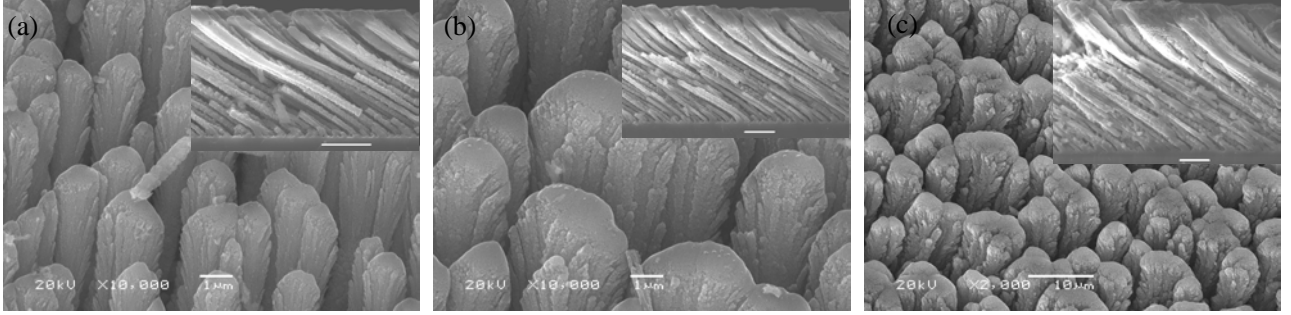


Fig. 1 SEM images of carbon rods structure synthesized at different temperature of (a)  $800^\circ\text{C}$ , (b)  $900^\circ\text{C}$ , (c)  $1000^\circ\text{C}$  and the corresponding cross section (insets). The scale bars are  $1\mu\text{m}$  for (a, b),  $10\mu\text{m}$  for (c) ( $5\mu\text{m}$  in the insets)

Schematic growth mechanisms illustrated in Fig. 2 were proposed to explain the different growth modes for tail-like carbon microrods prepared by HFPVD technique. Fig. 2 (a) is the sketch of the carbon stick filament connected to the copper electrodes,  $d_v$  and  $d_h$  is the vertical and horizontal distance between the filament and substrate, respectively,  $\alpha$  is the carbon source incident angle to the normal of substrate. The detailed parameters and data of fabricated samples are shown in table 1. Fig. 2 (b) demonstrates the growth process of the tail-like micro- and nano- hybrid carbon rods.  $\alpha'$  is the real angle of the rod to the normal.

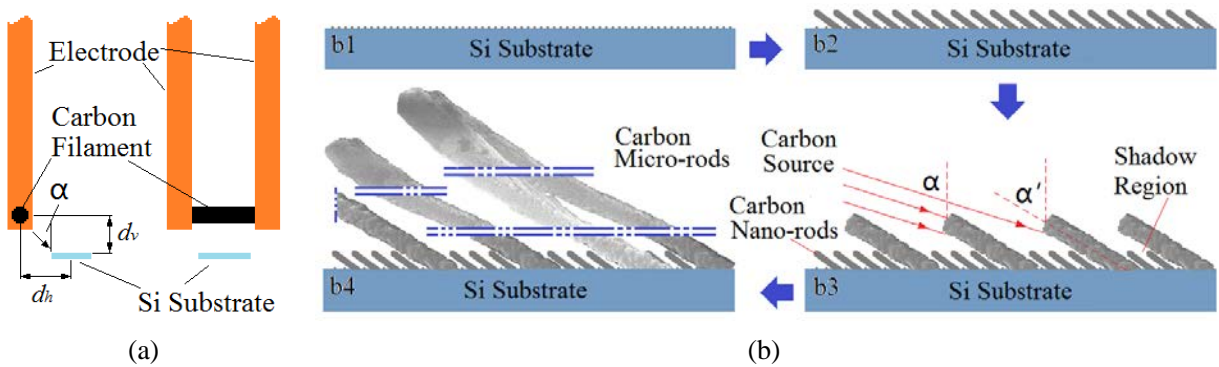


Fig. 2 Schematic illustration of (a) carbon filament and electrodes, (b) growth processes of tilted micro- and nano-hybrid carbon rods

Van der Drift model can be used to interpret the case of carbon rods as shown in Fig. 2(b). Random orientation nuclei were developed on the substrate at the initial stage of deposition (Fig. 2(b1)) yields a geometric shadow region [24, 25] where the subsequent incident flux cannot reach. Consequently, the oblique incident plasma flux is preferentially deposited on to the top of surface features, thus nanorods are formed (Fig. 2(b2)). With continued deposition, parts of rod grow up continuously to micro size, but others (shadow area) do not change, as shown in Fig. 2(b3). Shown in

Fig. 2(b4) is the final stage of deposition process that the tail-like microrods are developed. The sample surface has larger density than interior due to the larger size of the upper part than that of the beginning part, and the carbon rod-like structure has high surface area due to the coarse surface, which is good for hydrogen storage application.

Table 1

Sample	$d_v$ (mm)	$d_h$ (mm)	Substrate Temperature( $^{\circ}\text{C}$ )	$\alpha$ ( $^{\circ}$ )	$\alpha'$ ( $^{\circ}$ )	Thickness ( $\mu\text{m}$ )	Length ( $\mu\text{m}$ )	Beginning part dia. ( $\mu\text{m}$ )	End dia. ( $\mu\text{m}$ )
<i>a</i>	3.0	6.5	800	65	58.30	13.0	22.0-24.5	0.6-0.7	1.0-1.5
<i>b</i>	2.5	5.4	900	65	58.13	19.2	34.0-36.5	0.65-0.75	2.0-3.5
<i>c</i>	2.0	4.3	1000	65	57.68	25.3	44.0-47.0	0.7-1.0	3.0-4.5
<i>d</i>	4.0	10.0	600	68	60.22	5.5	10.9-11.1	0.35-0.5	0.8-1.0
<i>e</i>	4.0	11.0	600	70	61.35	4.6	8.9-9.6	0.38-0.6	0.6-1.1
<i>f</i>	4.0	12.5	600	72	62.46	3.9	8.2-8.5	0.3-0.5	0.6-0.9
<i>g</i>	4.0	14.0	600	74	63.54	3.3	6.9-7.4	0.35-0.45	0.5-0.9

In order to study the effect of incident angle of carbon source on sample structure, another four samples (*d*, *e*, *f*, *g*) were fabricated on Si at substrate temperature of  $600^{\circ}\text{C}$  with different incident angles, as shown in Fig. 3 (a), (b), (c), (d), respectively. The insets are FESEM images of their cross sections. Detailed parameters are summarized in table 1. Large-area uniform tail-like microrods, which have an average length of  $6.9\text{-}11.1\mu\text{m}$  and diameters  $0.3\text{-}0.6\mu\text{m}$  and  $0.6\text{-}1.2\mu\text{m}$  for the beginning part and the end part, hybridized with some  $130\text{-}150\text{nm}$  length,  $25\text{-}35\text{nm}$  diameter nanorods (Fig. 3 (c2)) were found in the four samples. The density of the microrod numbers decreases with increasing incident angle with respect to the normal. Fig. 3 (c1) shows the magnified SEM image of the selected area in sample *f* (Fig. 3 (c)) where the micro- and nanorods hybrid structure is clearly visible. Fig. 3 (c2) shows a shadow area with slant carbon nanorods structure.

Fig.3 (e) and (f) show the lower magnification FESEM images of sample *e* and *f*, respectively, which confirms the large-area uniform rod-like structure. It is inferred that well aligned carbon nanorods might be synthesized by controlling deposition duration and introducing inert gas to slow down the deposition rate.

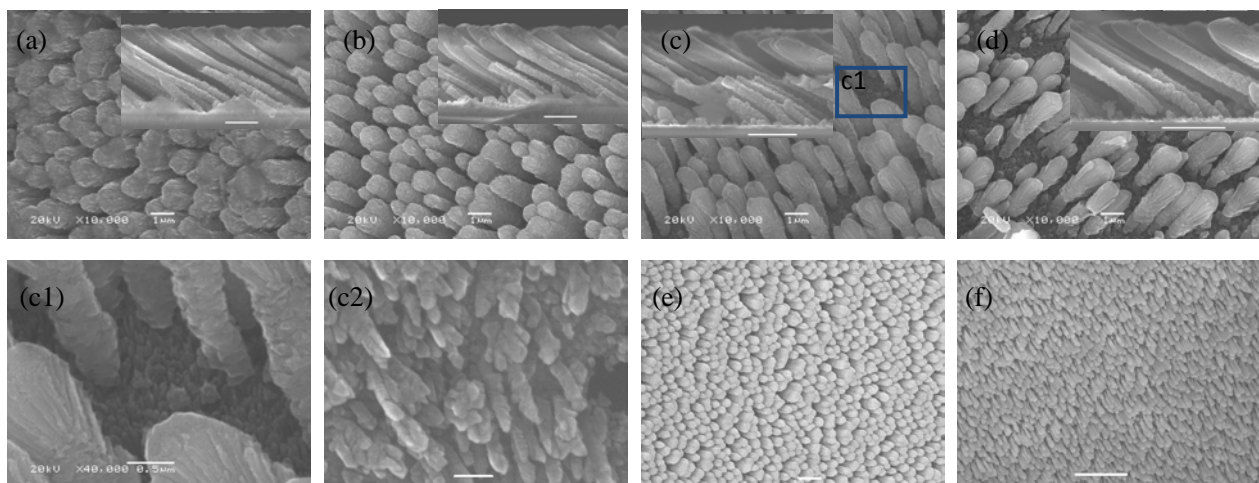


Fig. 3 (a-d) SEM images of carbon rods structure grown at 600°C with different incident angle. (c1, c2) Magnified SEM image and high magnification FESEM image of the shadow area in (c). (e, f) Lower magnification FESEM images of sample *e, f*. The scale bars are: (a-d) 1μm (2μm in the insets), (c1) 0.5μm, (c2) 100nm, (e) 2μm, (f) 10μm.

Fig. 4 shows the TED bright field (BF) images of single rods from the samples *a* and *f*, respectively. An end part of the tail-like micro-rod from the sample *a* with 5.9μm length, 1.1μm diameter is exhibited in Fig. 4 (a). Shown in Fig. 4 (b) is a plume-like structure of the rod from sample *f* with average diameter of 160nm and length of 1.4μm, which makes up the tail-like rod. Fig. 4 (c) is part of a tail-like rod from sample *f* with a length of 3.4μm and diameter of 0.4-0.6μm, the inset is its enlarged image of the marked area.

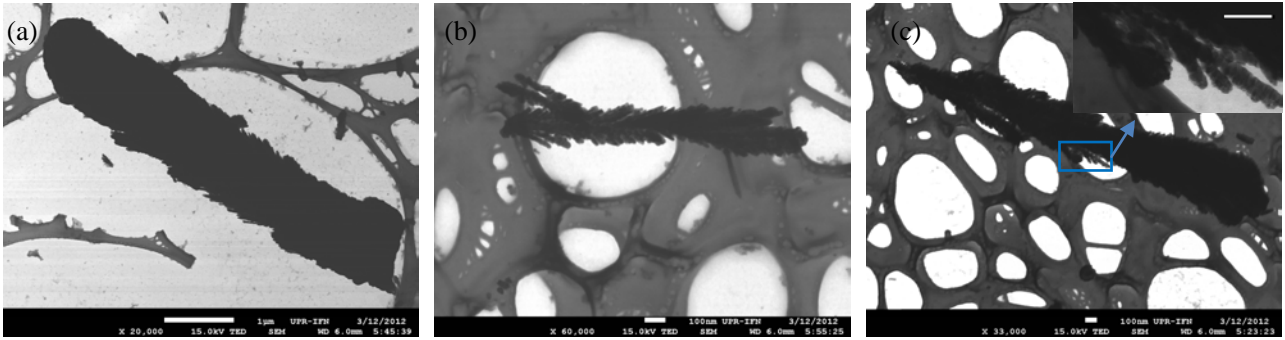


Fig. 4 TED BF images from (a) sample *a*, (b, c) sample *f*. The scale bars are: (a) 1μm, (b, c) 100nm (100nm in the inset)

Raman scattering spectra of the carbon structures were also obtained at room temperature by using a high resolution Jobin-Yvon T-64000 Triple-mate instrument with an excitation wavelength of 514.5nm (Ar<sup>+</sup> ion laser). A liquid nitrogen cooled charge-coupled device system was used to collect and process the scattered data.

Fig. 5 shows the Raman spectra of the synthesized carbon samples *a, b, c*, respectively. Characteristic graphite peaks are observed in the Raman spectra between 1000 and 2000 cm<sup>-1</sup>. The one at around 1345 cm<sup>-1</sup> (1344, 1341, 1345 cm<sup>-1</sup>, respectively) called D peak is associated with disorder-allowed zone edge modes of graphite that became Raman active due to the lack of long-range order in amorphous carbon-based materials. The G peak at around 1590 cm<sup>-1</sup> (1587, 1594, 1602 cm<sup>-1</sup>, respectively) corresponds to the G line associated with the optically allowed E<sub>2g</sub>-zone centre of crystalline graphite [26].



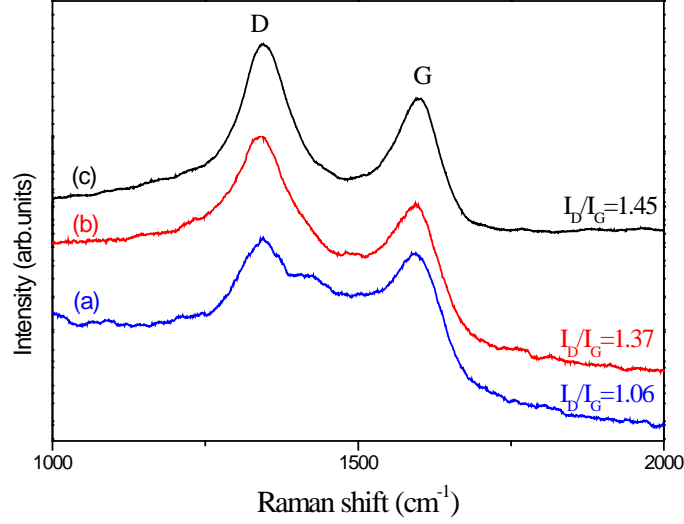


Fig. 5 Raman spectra of (a) samples *a*, (b) samples *b*, (c) samples *c*

It is also noted that the Raman signal ratio  $I_D/I_G$  increases from 1.06 to 1.45 following the substrate temperature from 800 to 1000 °C.

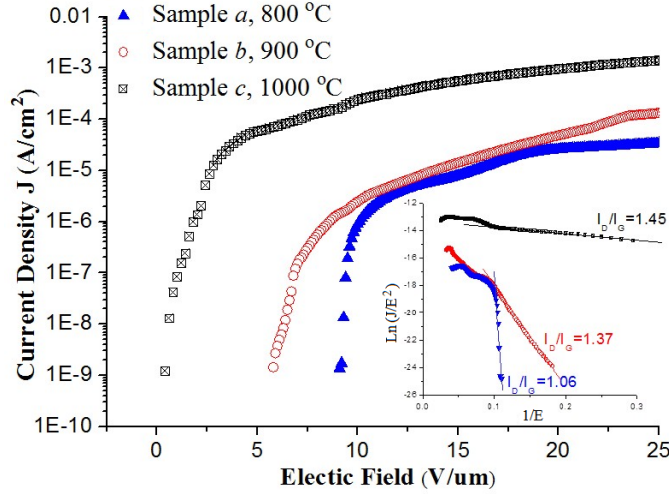


Fig. 6 The current versus electric field ( $I$ - $V$  curves) characteristics and Fowler–Nordheim (FN) plots (the inset) of samples *a*, *b*, *c*

The electrical properties of the samples *a*, *b*, *c* were investigated using a FE measurement system. Fig. 6 shows the field emission currents from the samples. The current density-electric field curve was obtained by recording each data point for 8 times with 250ms apart in order to reduce errors. In this work, electric current lower than  $1 \times 10^{-10}$  A was considered as the background noise level. The turn-on field ( $E_t$ ) is defined as the electric field necessary to emit 1nA current. The  $E_t$  of this three samples was 9.1 V/ $\mu$ m (sample *a*), 5.8 V/ $\mu$ m (sample *b*) and 0.4 V/ $\mu$ m (sample *c*). It should be mentioned that because of the effect of the Si substrate and the SiO<sub>2</sub> on its surface, the actual  $E_t$  value should be lower than what we measured. We repeated the FE measurement several times and the results showed a good consistency. The tail-like carbon rods deposited at 1000 °C has higher current density and lower turn-on field than others. These results clearly indicate that the FE characteristics of the samples are obviously improved under higher substrate temperature during the



deposition process.

According to the Fowler–Nordheim (FN) theory, the field emission current density  $J$  (emission current  $I$  /emission area  $A$ ) can be expressed as a function of the work function of the emission tip  $\Phi$ , the applied electric fields  $E$  and the field enhancement factor  $\beta$  [6, 27, 28] The FN equation is

$$J = A(\beta E)^2 / \Phi \exp(-B\Phi^{3/2} / \beta E),$$

where  $A$  and  $B$  are constants and their values are  $1.54 \times 10^{-6} \text{ A(eV)(V)}^{-2}$  and  $6.83 \times 10^3 \text{ (eV)}^{-2/3} \text{ V}\mu\text{m}^{-1}$ , respectively. The inset of Fig. 6 shows FN plots of the samples  $a$ ,  $b$ ,  $c$ . The fitted linear lines in the high voltage region indicate that electron emission follows the tunnelling mechanism, and from the slope of the fitted lines, the tail-like carbon micro- and nanorods hybrid structure at 1000 °C exhibits a higher value of field enhancement factor ( $\beta$ ) than the other two samples shown in figure 6 [29]. It can also be found that the FE characteristics of the carbon samples were enhanced together with the increase in the Raman signal ratio  $I_D/I_G$  from 1.06 to 1.45 shown in figure 6.

#### 4. Conclusion

In summary, we have demonstrated a simple route for synthesizing well aligned carbon micro- and nano- hybrid rod-like structures by using hot filament physical vapor deposition technique. The SEM images exhibit that micro-sized rods with different diameters are obtained for different substrate temperatures. The oblique angle and the density of the fabricated carbon rods are influenced by the carbon source incident angle. The carbon nanorods with diameter of 25-35nm are also obtained at the shadow areas. The turn-on field  $E_t$  of samples  $a$ ,  $b$ ,  $c$  is 9.1 V/ $\mu\text{m}$ , 5.8 V/ $\mu\text{m}$  and 0.4 V/ $\mu\text{m}$ . The field enhancement factor  $\beta$  increases following the increasing of substrate temperature from 800 to 1000 °C which is in accord with the Raman signal ratio  $I_D/I_G$ .

#### Acknowledgements

This work is partially supported by NSF-DMR (0706147). We would like to thank Dr. Carlos Cabrera and his staff Miss Christina for SEM measurements, Prof. R. Katiyar and his staff Mr. William's assistance of Raman measurements, Prof. Gerardo Morell for field emission measurements.

#### Reference

- [1] R.H. Baughman, A.A. Zakhidov, W.A. de Heer, Science 297 (2002) 787
- [2] A. Yamamoto, T. Tsutsumoto, Diam. Relat. Mater. 12 (2003) 1729
- [3] M.S. Wang, L.M. Peng, J.Y. Wang, C.H. Jin, Q. Chen, J. Phys. Chem. B 110 (2006) 9397
- [4] M.S. Wang, J.Y. Wang, L.M. Peng, Appl. Phys. Lett. 88 (2006) 243108
- [5] H.X. Zhang, P.X. Feng, Appl. Surf. Sci. 255 (2009) 5939
- [6] R.C. Che, M. Takeguchi, M. Shimojo, K. Furuya, J. Phys.: Conf. Ser. 61 (2007) 200
- [7] R. Strobel, J. Garche, P.T. Moseley, L. Jorissen, G. Wolf, J. Power Sources 159 (2006) 781
- [8] A.C. Dillon, M.J. Heben, Appl. Phys. A 72 (2001) 133
- [9] M.Y. Teng, K.S. Liu, H.F. Cheng, I.N. Lin, Diam. Relat. Mater. 12(2003) 450
- [10] M. Ishihara, M. Suzuki, T. Watanabe, T. Nakamura, A. Tanaka, Y. Koga, Diam. Relat. Mater. 14 (2005) 989
- [11] H.X. Zhang, P.X. Feng, P. Jin, V.I. Makarov, L. Fonseca, G. Morell, B.R. Weiner, Appl. Phys. Lett. 95 (2009)

- [12] H.X. Zhang, P.X. Feng, V.I. Makarov, L. Fonseca, G. Morell, B.R. Weiner, J. Phys. D: Appl. Phys. 42 (2009) 035409
- [13] I.C. Chen, L.H. Chen, X.R. Ye, C. Daraio, S. Jin, C.A. Orme, A. Quist, R. Lal, Appl. Phys. Lett. 88 (2006) 153102
- [14] J.B. Chen, C.W. Wang, J. Wang, Y. Li, R.S. Guo, B.H. Ma, F. Zhou, W.M. Liu, Appl. Surf. Sci. 256 (2009) 39
- [15] J.J. Schneider, N.I. Maksimova, J. Engstler, R. Joshi, R. Schierholz, R. Feile, Inorg. Chim. Acta 361 (2008) 1770
- [16] G.F. Zou, J. Lu, D.B. Wang, L.Q. Xu, Y.T. Qian, Inorg. Chem. 43 (2004) 5432
- [17] X.J. Wang, J. Lu, Y. Xie, G.A. Du, Q.X. Guo, S.Y. Zhang, J. Phys. Chem. B 106 (2002) 933
- [18] D.X. Ye, T. Karabacak, B.K. Lim, G.C. Wang, T.M. Lu, Nanotechnology 15 (2004) 817
- [19] H.X. Zhang, P.X. Feng, J. Phys. D: Appl. Phys. 42 (2009) 025406
- [20] P.X. Feng, X.P. Wang, H.X. Zhang, B.Q. Yang, Z.B. Wang, A. Gonzalez-Berrios, G. Morell, B. Weiner, J. Phys. D: Appl. Phys. 40 (2007) 5239
- [21] H.X. Zhang, B.Q. Yang, P.X. Feng, J. Nanomater. (2008) 957935
- [22] X.P. Wang, B.Q. Yang, H.X. Zhang, P.X. Feng, Nanoscale Res. Lett. 2 (2007) 405
- [23] H.X. Zhang, P.X. Feng, J. Phys. D: Appl. Phys. 41 (2008) 155425
- [24] J. Chu, X.Y. Peng, M. Sajjad, B.Q. Yang, P.X. Feng, Thin Solid Films 520 (2012) 3493
- [25] C. Gaire, F. Tang, G.C. Wang, Thin Solid Films 517 (2009) 4509
- [26] H.Y. Li, Y.C. Shi, P.X. Feng, Appl. Phys. Lett. 89 (2006) 142901
- [27] Y. Ryu, Y. Tak, K. Yong, Nanotechnology 16 (2005) S370
- [28] Field electron emission. From Wikipedia: [http://en.wikipedia.org/wiki/Field\\_electron\\_emission](http://en.wikipedia.org/wiki/Field_electron_emission)
- [29] C.Y. Su, Z.Y. Juang, Y.L. Chen, K.C. Leou, C.H. Tsai, Diam. Relat. Mater. 16 (2007) 1393